



# Hypomethylation-Mediated Upregulation of *NFE2L3* Promotes Malignant Phenotypes of Clear Cell Renal Cell Carcinoma Cells

Xuehua Hou<sup>1</sup> · Qin Liao<sup>1</sup> · Ying Wu<sup>1</sup> · Luo Wang<sup>1</sup> · Jianfeng Zhao<sup>2</sup> · Xuhui Liao<sup>3</sup>

Received: 14 September 2022 / Accepted: 15 March 2023 / Published online: 18 April 2023  
© The Author(s), under exclusive licence to Springer Science+Business Media, LLC, part of Springer Nature 2023

## Abstract

This work aimed to study the effect of NFE2 like bZIP transcription factor 3 (*NFE2L3*) on clear cell renal cell carcinoma (ccRCC) cells and whether *NFE2L3* expression was mediated by DNA methylation. Twenty-one ccRCC patients were collected. The gene methylation and expression data of TCGA-KIRC were accessed from TCGA. Candidate methylation driver genes were identified by “MethylMix” package, and finally, *NFE2L3* was selected as the target gene. The methylation of *NFE2L3* was assayed by Ms PCR and QMSP. mRNA level of *NFE2L3* was analyzed by qRT-PCR. Protein level of *NFE2L3* was measured by Western blot. Demethylation was performed with methylation inhibitor 5-Aza-2'-deoxycytidine (5-Aza-CdR). Proliferative, migratory, and invasive abilities of ccRCC cells were assayed via cell colony formation assay, scratch healing assay, and transwell assay, respectively. Analysis of TCGA database presented that DNA hypomethylation occurred in the *NFE2L3* promoter region in ccRCC tissues. *NFE2L3* was significantly upregulated in ccRCC tissues and cells. Its expression in cells treated with 5-Aza-CdR was proportional to the concentration of methylation inhibitor. In cell function experiments, overexpressing *NFE2L3* or demethylation could stimulate proliferation, migration, and invasion abilities of ccRCC and normal cells. 5-Aza-CdR treatment rescued repressive impact of knockdown *NFE2L3* on malignant phenotypes of ccRCC and normal cells. DNA hypomethylation could induce high expression of *NFE2L3* and facilitate malignant phenotypes of ccRCC cells. These results may generate insights into ccRCC therapy.

**Keywords** *NFE2L3* · ccRCC · Methylation · Proliferation · Migration

## Introduction

In developed countries, kidney cancer is a relatively common cancer [1] with treatment difficulties and poor prognosis. More than 90% of kidney cancer is renal cell carcinoma (RCC) from renal tubular structure, and the rest less than 10% are transitional cell carcinoma originating from cells lining the renal pelvis and ureter [2, 3]. Clear cell RCC

(ccRCC) is the most common subtype of RCC, which comprises about 75% of all RCCs. Since ccRCC is not sensitive to traditional chemotherapy, the research about targeted therapies for this cancer is attracting increasing attention from doctors and scholars. In order to further study the targeted therapies of ccRCC, we should have a deep understanding of the internal mechanism affecting its occurrence and development.

NFE2 like bZIP transcription factor 3 (*NFE2L3*) was first discovered in 1999 and reported to be involved in Wnt signaling pathway and oxidative stress [4]. *NFE2L3* plays an imperative part in regulating expression of developmental-related genes [5–7] and participates in cell differentiation, inflammation, and carcinogenesis [8–10]. The function of *NFE2L3* varies in the carcinogenesis process of different cancer types. For example, Chevillard et al. [10] found that deletion of *NFE2L3* predisposed mice to lymphoma, indicating that *NFE2L3* inhibited lymphomas. Chowdhury et al. [11] confirmed that *NFE2L3* facilitated cell proliferation via upregulating UHMK1 in colon cancer. Therefore, *NFE2L3*

✉ Xuhui Liao  
xvhuiliao@163.com

<sup>1</sup> Department of Oncology, Shulan(Hangzhou)Hospital Affiliated to Zhejiang Shuren University Shulan International Medical College, Hangzhou 310022, Zhejiang, China

<sup>2</sup> Neurosurgery, Xiangshan First People's Hospital Medical and Health Group, Xiangshan 315700, Zhejiang, China

<sup>3</sup> Department of Pathology, Lishui People's Hospital, No. 15, Volkswagen Street, Liandu District, Lishui 323000, Zhejiang, China

is a colon cancer-promoting factor. However, the effect of *NFE2L3* on ccRCC has not been clearly studied, and it is worthy of further discussion.

Hypomethylation of oncogenes and hypermethylation of tumor suppressors have been extensively regarded as important regulatory factors in the occurrence and progression of cancer [12]. DNA methylation means adding a methyl group to 5' cytosine of a CG dinucleotide, which is called CpG for short. Aberrant CpG island methylation occurs in gene promoter regions at different stages of tumor development, resulting in transcriptional silencing and aberrant levels of varying key genes [13]. In ccRCC, Shen et al. [14] proved that DNA hypomethylation in the 3'UTR region leads to high expression of BHLHE41, thereby enhancing the bioactivity of tumor cells. Kang H W et al. [15] also demonstrated that DNA methylation is associated with progression of ccRCC. It followed that DNA methylation could not only affect the development of ccRCC but also affect the prognosis of patients. *NFE2L3* has been recently labeled as a new DNA methylation-driven gene in human ccRCC, exhibiting a hypomethylated state in the ccRCC cancer cohort [16]. However, what kind of biological function *NFE2L3* plays in ccRCC and whether influence of *NFE2L3* on biological function of ccRCC cells is related to its hypomethylation status are still underexplored.

This study attempts to explore influence of *NFE2L3* on malignant progression of ccRCC cells and whether this process is mediated by hypomethylation, thus providing theoretical support for the development of new ccRCC treatment options.

## Materials and Methods

### Bioinformatics Methods

The methylation data (Illumina human methylation 450, Normal: 160, Tumor: 325) and expression data (Normal: 72, Tumor: 539) of TCGA-KIRC were downloaded from TCGA database on June 15th, 2020. The “limma” package was used to normalize the methylation data. The annotation files were downloaded from the GENECODE (<https://www.genecodegenes.org/human/>) database to annotate the ENsembl ID to separate mRNA. The average expression of duplicated genes was computed. Genes with an average expression of less than 1 were filtered out, and the ‘edgeR’ package was used for normalization and differential analysis. Genes with average methylation of 0 were filtered out, and the “limma” package was used to normalize the methylation data. The “MethylMix” was applied to select candidate methylation driver genes ( $\log_2FC > 0.3$ ,  $\text{adjust}P < 0.05$ ,  $\text{Cor} < 0.3$ ). Ultimately, *NFE2L3* was determined to be the target gene. The tumor samples were separated into two groups according

to median *NFE2L3* methylation level in tumor tissues, and “survival” package was applied for survival analysis. Meanwhile, survival analysis was performed in combination with the expression level of *NFE2L3* gene. Then, Chi-square test was employed to ascertain correlation between *NFE2L3* methylation level and clinical practice.

Similarly, survival analysis of *NFE2L3* was conducted, and the correlation between *NFE2L3* and clinical practice was explored. Finally, 539 tumor samples were separated into two groups (high expression: 270, low expression: 269) according to median *NFE2L3* level. Overall survival rates of patients in the two groups were compared. Survival rate was assayed using Kaplan–Meier method and log-rank test. The “c2.cp.kegg.v7.0.symbols.gmt” data were downloaded as a reference gene set from MSigDB (<http://software.broadinstitute.org/gsea/msigdb/index.jsp>). Gene Set Enrichment Analysis (GSEA) for single-gene was performed using GSEA 4.0.1 software.

### Patients and Tissue Collection

From July 2021 to March 2022, 21 pairs of ccRCC tissue and adjacent normal tissue from patients who underwent ccRCC surgery in People’s Hospital of Lishui City were collected. All patients were confirmed by two or more pathologists and had not treated with any anticancer therapy before sampling. The collected samples were snap-frozen in liquid nitrogen for use in subsequent experiments. Written informed consent was obtained from every participant. This study was approved by the Ethics Committee of People’s Hospital of Lishui City.

### Cell Line Culture

Human renal proximal tubular epithelial cell line RPTEC (BNCC340070) and four human ccRCC cell lines, LoMet-ccRCC (BNCC101803), Caki-1 (BNCC100682), Caki-2 (BNCC101647), and 769-P (BNCC100976) were offered by BeNa Culture Collection (BNCC, China). For cell biological function experiments, Caki-1 was maintained in McCoy’s 5A Media (BNCC338366) containing 10% FBS, while other cells were kept in Dulbecco’s modified Eagle’s medium (Gibco, USA) plus 10% fetal bovine serum (FBS, BNCC341830). The culture conditions were 37 °C and 5% CO<sub>2</sub>.

### Cell Transfection

Cells in logarithmic phase were utilized for transfection. The oe-*NFE2L3* (*NFE2L3* overexpression system constructed by pcDNA3.1), oe-NC (control group of *NFE2L3* overexpression system constructed by pcDNA3.1), sh-NC (control group of *NFE2L3* knockdown system), and sh-*NFE2L3*

(knockdown system of *NFE2L3*) were all purchased from Sangon Biotech (China). Plasmids were diluted using serum-free McCoy's 5A Media. 4  $\mu$ L lipofectamine 2000 (Invitrogen, USA) reagent was supplemented to 50  $\mu$ L of McCoy's 5A Media. The diluted plasmid solution was mixed with the prepared lipofectamine solution, followed by shaking and 20 min of standing. After cells were rinsed twice with PBS, the above mixture was added to cells in each group. After 48 h of transfection, cells were harvested for the follow-up experiments.

### DNA Extraction and Ms PCR

Genomic DNA was isolated by protease K method. The cells were digested with DNA digestion buffer (pH 8.0, 25 mM EDTA, 10 mM Tris-Cl, 100  $\mu$ g/mL protease K, 1% SDS) and isolated with phenol/chloroform. The EpiTect bisulfite kit (Qiagen, Germany) was used for DNA bisulfite conversion. Online software (MethPrimer) was adopted for primer design, and primer sequences are shown in Table 1. Methylation analysis of hydrogenated DNA was performed by PCR. The thermal cycling parameters were 95 °C for 5 min; 35 cycles of 95 °C for 30 s, 60 °C for 30 s and 72 °C for 40 s; and 72 °C for 5 min. Ms PCR products were separated by 2% agarose gel, stained with ethidium bromide, and analyzed by nucleic acid gel imaging system (BIO-RAD, USA).

### TaqMan Quantitative Methylation-Specific PCR (QMSP)

The methylation primers for QMSP were the same as Ms PCR. The reaction volume was 10  $\mu$ L (5  $\mu$ L of 2 $\times$  Master Mix, 2.5  $\mu$ L of BS-DNA (10 ng/ $\mu$ L), 0.3  $\mu$ L of forward primer and 0.3  $\mu$ L of reverse primer (10  $\mu$ mol/L), 0.4  $\mu$ L of probe (5  $\mu$ mol/L), and 1.5  $\mu$ L of ddH<sub>2</sub>O). Three parallel wells were set for each DNA sample. PCR detection was done using the ABI PRISM® 7900HT Sequence Detection System. QMSP cycling program was: 95 °C for 10 min, 50 cycles of 95 °C for 15 s, and 60 °C for 1 min. ACTB gene was utilized as a methylation reference gene. Relative methylation levels of *NFE2L3* DNA were normalized to ACTB. *NFE2L3* was considered hypomethylated

when its methylation level relative to that of ACTB gene in ccRCC tissues was half that of paired adjacent normal tissue samples.

### Total RNA Extraction and qRT-PCR

Total RNA was isolated from cells with TRIzol reagent (Sigma, USA). cDNA synthesis was performed using PrimeScript RT reagent Kit (Takara, Japan). qPCR was carried out using SYBR premixed Ex Taq (Takara, Japan) and Vii-ATM 7 real-time PCR system (Applied Biosystems, USA). PCR conditions were 95 °C for 30 s, 30 cycles of 95 °C for 5 s, 60 °C for 30 s and 95 °C for 15 s, 60 °C for 30 s and 95 °C for 15 s. Relative mRNA expression was calculated using  $2^{-\Delta\Delta C_t}$  method with GAPDH as reference. Primers for *NFE2L3* and GAPDH were bought from Sangon Biotech (China). The primer sequences are presented in Table 2.

### Western Blot

Total proteins were isolated with RIPA lysis buffer and extraction buffer (Thermo Fisher Scientific, USA). The protein concentration was assayed by BCA kit (Thermo Fisher Scientific, USA). The proteins were concentrated and divided via SDS-PAGE gel (Bio-Rad, USA), then blotted onto PVDF membrane, and blocked with 5% skim milk for 1 h. Afterward, membrane was incubated overnight with primary antibodies and cultured for 1 h with secondary antibody. Images were programmed using standard Western blotting techniques on Bio-Rad ChemiDoc MP imaging system (Hercules, USA). Primary antibodies were rabbit anti-NFE2L3 (1:1000, AP19864B, APCEPTA, USA) and rabbit anti-GAPDH (1: 2500, PA1-988, Thermo Fisher

**Table 1** Ms PCR primer sequences

Gene	Primer	GC (%)	Size (bp)	T <sub>m</sub> (°C)	
NFE2L3 M	Forward Primer	5'-ATGTGAAATTTTCG AATTTTATACGA-3'	40	25	58.18
	Reverse Primer	5'-GAAAAACCTAAC AACTTACAACGAA-3'	72	25	58.03
NFE2L3 U	Forward Primer	5'-ATGTGAAATTTT GAATTTTATATGA-3'	40	25	54.15
	Reverse Primer	5'-AAAAAACCTAAC AACTTACAACAAA-3'	72	25	55.71

**Table 2** qRT-PCR primer sequences

Gene	Sequence
NFE2L3	Forward primer 5'-GGGGAAGAGGAGAAGGCAC-3'
	Reverse primer 5'-GGCTGACACCCTTTCTTCATT-3'
GAPDH	Forward primer 5'-GAAGGTGAAGGTCGGAGTC-3'
	Reverse primer 5'-GAAGATGGTGATGGGATTTC-3'

Scientific, USA). Secondary antibody was goat anti-rabbit IgG (0.25 µg/mL, A32731, Thermo Fisher Scientific, USA).

### Demethylation Assay

ccRCC cells with low or deficient *NFE2L3* expression and human renal proximal tubular epithelial cells (RPTECs) and ccRCC cells (Caki-1, Caki-2, 769-P, LoMet-ccRCC) were inoculated in a 6 cm petri dish at a concentration of  $5 \times 10^5$  cells per dish. After 24 h, 5-Aza-2'-deoxycytidine (5-Aza-CdR, Selleckchem, USA) at doses of 0, 0.5, 1, 2.5, 5, and 10 µM was added for 72 h, then RNA and proteins were extracted.

### Colony Formation Assay

ccRCC cells of different groups were plated into 6-well plates ( $1 \times 10^3$  cells/well). The culture was finished when the dilute cell colonies were visible to the naked eye. ccRCC cells were fixed with 75% ethanol for 30 min, and then dyed with 0.5% crystal violet solution for statistics. Five visual fields were randomly selected for counting. Each assay was repeated three times.

### Scratch Healing Assay

ccRCC cells of different groups were plated into 6-well plates ( $1 \times 10^5$  cells/well) until they covered bottom of the plate. A 200 µL sterile pipette tip was utilized to create the wound on cell monolayer. Following rinsing with phosphate-buffered saline (PBS) three times, medium was cultured at 37 °C without FBS for 24 h. The cells were photographed at 0 and 24 h after wound creation. Cell migration distance was measured after image acquisition. Migration rate = (0 h scratch width – 24 h scratch width)/0 h scratch width. Five visual fields were randomly selected to count migrated cells. The experiment was repeated three times.

### Cell Invasion Assay

Briefly, cell invasion assay means using Transwell Chambers (8 µm, BD Biosciences, USA) to study invasion. The chambers were placed in a 24-well plate, and  $2 \times 10^4$  cells suspended in 100 µL serum-free medium were placed in the bottom chamber precoated with matrix. 600 µL medium containing 10% FBS was added to the well plate as the inducer. After incubation for 24 h, cells on the upper surface were removed, and those invading to the lower surface of the membrane were fixed with methanol, stained with 0.1% crystal violet at 37 °C for 30 min, and rinsed with PBS twice. Cells were photographed under a microscope in three separate areas and counted for staining. Five visual

fields were randomly selected to count invading cells. The experiment was repeated three times.

### Data Processing

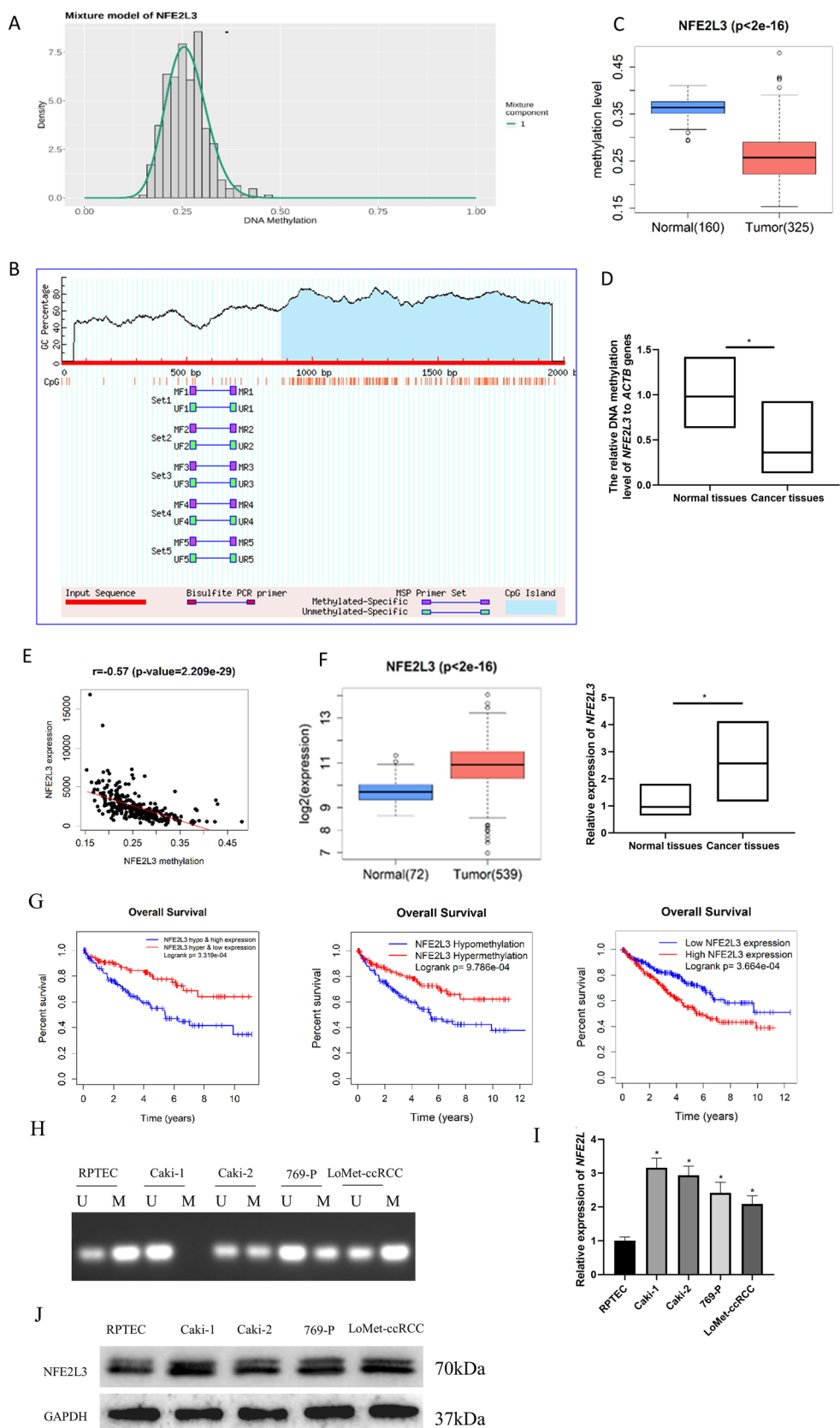
All results were statistically analyzed by SPSS21.0. Quantitative data were presented as mean ± standard deviation. *T*-test was utilized for hypothesis test for inter-group comparison. Before hypothesis testing, normality analysis and homogeneity of variance test should be carried out for each group of data. Non-parametric test should be used for data that do not conform to normal distribution. When  $p < 0.05$ , there was a prominent statistical difference. When  $p < 0.01$ , there was an extremely significant statistical difference.

## Results

### *NFE2L3* Shows Hypomethylation and High Expression in ccRCC

To investigate the influence of *NFE2L3* methylation and expression on ccRCC, we firstly selected candidate methylation driver genes by MethylMix. The result showed that there was methylation modification of *NFE2L3* in cancer tissues (Fig. 1A). Then, we used software ([www.urogene.org/](http://www.urogene.org/)) to search the Human Genome Database for CpG islands in the *NFE2L3* gene promoter and found that the CpG islands located in 1070 bp (875–1944) behind the promoter. This indicated that the expression of *NFE2L3* was related to abnormal methylation (Fig. 1B). It was indicated that the DNA in the *NFE2L3* promoter region was hypomethylated. Then, we predicted the methylation levels of *NFE2L3*. In TCGA database, methylation levels in the *NFE2L3* promoter region were substantially decreased in tumor tissues in relevant to normal tissues (Fig. 1C). We collected tumor tissues and corresponding normal adjacent tissues from ccRCC patients for validation. We found that *NFE2L3* was stimulated in tumor tissues in relevant to normal tissues (Fig. 1D). MethylMix analysis showed a substantial negative association between *NFE2L3* methylation level and its gene expression (Fig. 1E). By bioinformation analysis and qRT-PCR, we manifested that *NFE2L3* was highly expressed in ccRCC patient tissues (Fig. 1F). Combined with the methylation and expression levels of *NFE2L3*, we found that survival time of patients with hypermethylation and low expression of *NFE2L3* was significantly longer than that of patients with hypomethylation and high expression of *NFE2L3*. In addition, separate survival analyses of *NFE2L3* gene expression level and methylation level also showed that high expression or hypomethylation of *NFE2L3* predicted a poor prognosis (Fig. 1G). It was indicated that the low expression of *NFE2L3* mediated by DNA methylation was significantly

**Fig. 1** *NFE2L3* is hypomethylated in ccRCC. **A** For the mixture model of *NFE2L3* methylation, the abscissa represents the degree of methylation; the ordinate represents the number of methylated samples; the histogram represents the methylation distribution of the tumor group; the peak of the curve indicates the mean level of methylation distribution in the tumor group; the bold horizontal line represents the mean level of methylation distribution in the normal group; **B** Methylation status of *NFE2L3* CpG sites in TCGA dataset; **C** Boxplot of *NFE2L3* methylation level in normal group (blue) and tumor group (red); **D** The methylation level of *NFE2L3* was measured by QMSP in 21 pairs of ccRCC patient tumor tissues and adjacent normal tissues; **E** Correlation between methylation level and expression level of *NFE2L3*; **F** Boxplot of *NFE2L3* expression level in normal group (blue) and tumor group (red), and the mRNA expression level of *NFE2L3* in 21 pairs of ccRCC patient tumor tissues and adjacent normal tissues was measured by qRT-PCR; **G** Survival curve of patients with different *NFE2L3* methylation and expression levels (red line for hypermethylation and low expression group, and blue line for hypomethylation and high expression group); Survival curve of patients with different *NFE2L3* gene expression (red line for high expression group, and blue line for low expression group); Survival curve of patients with different *NFE2L3* methylation levels (red line for hypermethylation group, blue line for hypomethylation group); **H** Ms PCR detection results of methylation in normal cells and ccRCC cells (U: unmethylated, M: methylated); **I** qRT-PCR detection result of mRNA expression of *NFE2L3* in each cell line; **J** Western blot detection result in protein expression of *NFE2L3* in each cell line. (\* denotes  $p < 0.05$ )



conductive to the prognosis of patients. Hypomethylation of *NFE2L3* in ccRCC was correlated with high *NFE2L3* gene expression and a poor prognosis.

The result of Ms PCR detection in RPTEC and LoMet-ccRCC, Caki-1, Caki-2 and 769-P cells were shown in Fig. 1H. When fluorescence was only displayed under U band, we believed that methylation did not occur. When fluorescence was displayed under M band or under both M and U bands, methylation or partial methylation was considered. Therefore, we found that the methylation degree of RPTEC cells was higher than that of ccRCC cells. Among all ccRCC cells, the most methylated cells were LoMet-ccRCC cells and the lowest were Caki-1 cells. *NFE2L3* level in ccRCC cells and RPTEC cells were assessed. Notably, qRT-PCR detection illustrated that *NFE2L3* mRNA level in all ccRCC cells was higher than in RPTEC, (Fig. 1I) and the same trend was observed in the result of Western blot (Fig. 1J). In conclusion, *NFE2L3* presented hypomethylation and high expression in ccRCC cells.

### Hypomethylation of *NFE2L3* Promoter Region Mediates High Gene Expression

To further confirm that the expression of *NFE2L3* in ccRCC was mediated by methylation, we then treated ccRCC cells and human renal proximal tubular epithelial cell line RPTEC with 5-Aza-CdR (demethylating drugs). The results presented that *NFE2L3* mRNA expression in RPTEC, LoMet-ccRCC, Caki-2, and 769-P cell lines increased with the increase of 5-Aza-CdR concentration and did not increase after a certain concentration reached a plateau. Meanwhile, the expression level of *NFE2L3* mRNA in RPTEC cell line

was higher than that in ccRCC cell lines. In Caki-1 cell line, the impact of demethylation treatment on *NFE2L3* mRNA expression was not obvious. This may be associated with methylation degree of *NFE2L3* in different cell lines (Fig. 2A). As such, Western blot presented that *NFE2L3* protein level in human renal proximal tubular epithelial cell line RPTEC and all ccRCC cells (Caki-1, Caki-2, 796-P, LoMet-ccRCC) increased with the increase of 5-Aza-CdR concentration (Fig. 2B). Thus, the degree of demethylation was proportional to expression of *NFE2L3*.

### *NFE2L3* Overexpression Promotes Malignant Phenotypes of ccRCC Cells

Substantial evidence suggests that *NFE2L3* serves as a modulator of proliferation and migration/invasion in a variety of cancers [17–19]. In the following step, we investigated the regulatory role of *NFE2L3* in ccRCC cells and RPTEC cells. As the expression of *NFE2L3* in Caki-1 cell line was the highest and that in LoMet-ccRCC cell line was the lowest among the four ccRCC cell lines, LoMet-ccRCC was selected for *NFE2L3* overexpression treatment and Caki-1 for *NFE2L3* knockdown treatment. First, *NFE2L3* was overexpressed in the LoMet-ccRCC and RPTEC cells, which were divided into oe-NC group and oe-*NFE2L3* group. Transfection efficiency was assayed via qRT-PCR and Western blot (Fig. 3A–B, Supplementary Fig. 2A). *NFE2L3* mRNA and protein levels in ccRCC and RPTEC cells were noticeably increased after oe-*NFE2L3* treatment, indicating the success of transfection. Then, we detected the change in methylation state of *NFE2L3* gene in LoMet-ccRCC and RPTEC cells after transfection. The results showed that

**Fig. 2** Hypomethylation of *NFE2L3* promoter region mediates high gene expression. **A** qRT-PCR detected mRNA expression of *NFE2L3* in ccRCC cells and RPTEC cells treated with methylation inhibitor 5-Aza-CdR; **B** Western blot detected the protein expression of *NFE2L3* in RPTEC cells and ccRCC cells treated with methylation inhibitor 5-Aza-CdR

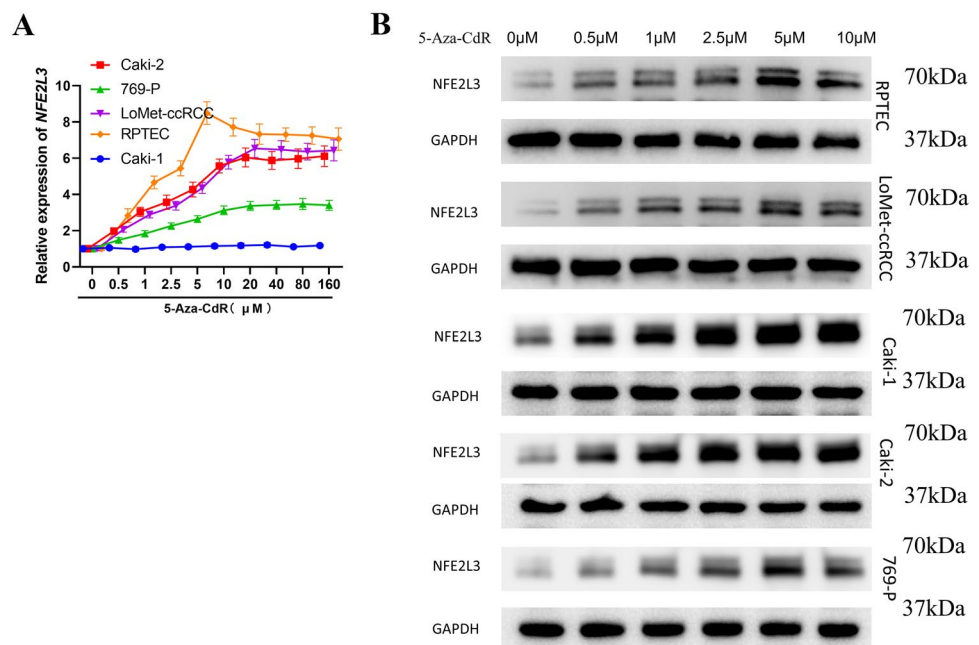
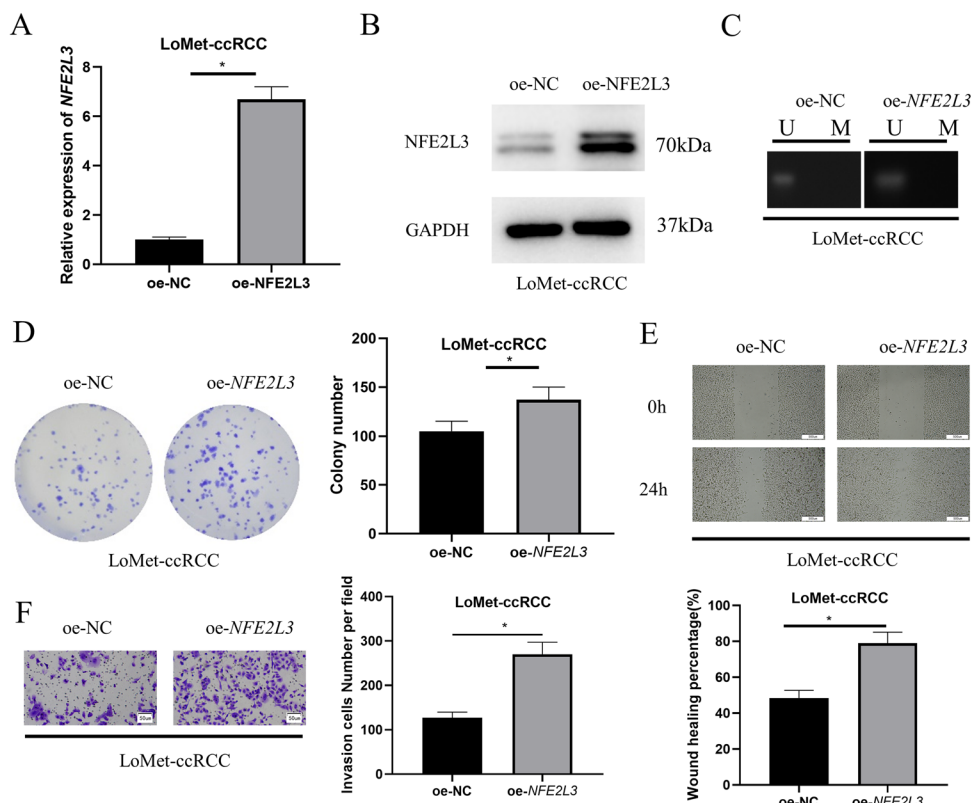


**Fig. 3** Overexpression of *NFE2L3* promotes malignant phenotypes of LoMet-ccRCC cells. **A** qRT-PCR detected transfection efficiency of LoMet-ccRCC cells; **B** Western blot detected the protein expression of *NFE2L3* in transfected LoMet-ccRCC cells; **C** Change in methylation state of *NFE2L3* gene in ccRCC cell line LoMet-ccRCC after transfection; **D** Cell colony formation assay detected proliferative ability of LoMet-ccRCC cells; **E** Scratch healing assay detected the migratory ability of LoMet-ccRCC cells ( $\times 40$ ); **F** Cell invasion assay detected the invasive ability of LoMet-ccRCC cells ( $\times 100$ ). (\* denotes  $p < 0.05$ )



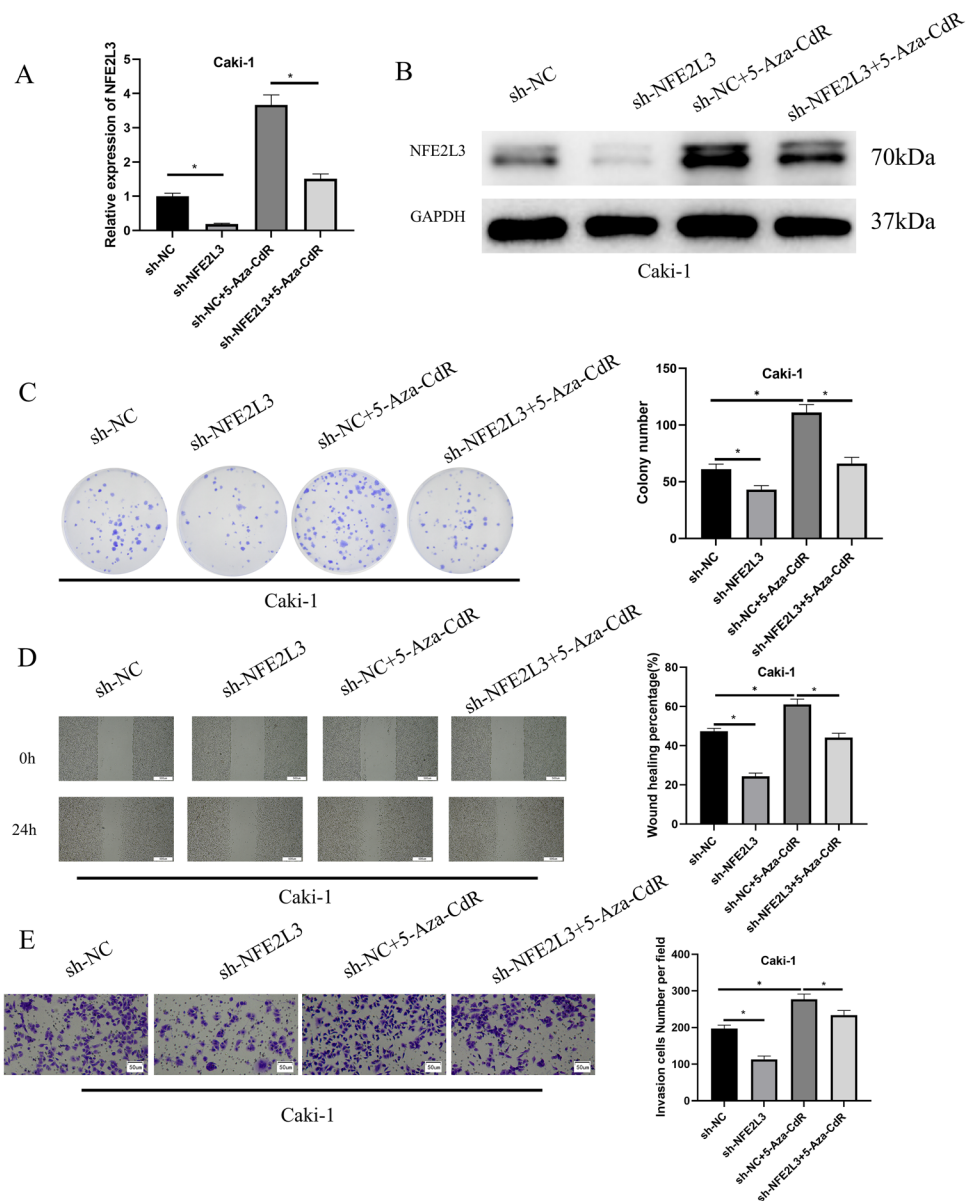
methylation state of *NFE2L3* in *oe-NFE2L3* group was lower than that in *oe-NC* group (Fig. 3C, Supplementary Fig. 2B). Meanwhile, we designed multiple cell function experiments to evaluate the malignant behaviors of cells. Colony formation assay illustrated that overexpression of *NFE2L3* could notably enhance LoMet-ccRCC and RPTEC cell proliferative property (Fig. 3D, Supplementary Fig. 2C). Furthermore, tumor cells with overexpressed *NFE2L3* were substantially enhanced in both cell migration and invasion, as revealed by wound healing assay (Fig. 3E, Supplementary Fig. 2D) and Transwell assay (Fig. 3F, Supplementary Fig. 2E). These suggested that *NFE2L3* overexpression could facilitate the development of ccRCC cells.

### Repression of Methylation Attenuates the Tumor Suppressive Effect Caused by *NFE2L3* Knockdown

Since high level of *NFE2L3* was mediated by its hypomethylation, overexpression of *NFE2L3* could facilitate the growth of ccRCC cells in vitro and thus, we used 5  $\mu$ M/L 5-Aza-CdR to explore whether *NFE2L3* regulates gene expression through demethylation and thereby affects malignant progression of ccRCC. In this respect, we first constructed two sh-*NFE2L3* plasmids and examined the transfection efficiency by qRT-PCR (Supplementary

Fig. 1). We selected sh-*NFE2L3*-1 with higher transfection efficiency for subsequent experiments and nominated it as sh-*NFE2L3*. Cells expressing sh-NC or sh-*NFE2L3* were then treated with 5-Aza-CdR, respectively. qRT-PCR and Western blot denoted that *NFE2L3* mRNA and protein levels were substantially decreased in the sh-*NFE2L3* group and increased noticeably in 5-Aza-CdR group, and 5-Aza-CdR could restore *NFE2L3* expression (Fig. 4A–B, Supplementary Fig. 3A–B). The results of cell colony formation assay presented that in comparison with the control, cell colony formation of Caki-1 and Caki-2 cells transfected with sh-*NFE2L3* was markedly reduced, and 5-Aza-CdR treatment notably increased cell colony formation ability of Caki-1 and Caki-2 cells. Additionally, 5-Aza-CdR rescued repressive impact of *NFE2L3* knockdown on growth of Caki-1 and Caki-2 cells (Fig. 4C, Supplementary Fig. 3C). As such, wound healing assay (Fig. 4D, Supplementary Fig. 3D) and Transwell (Fig. 4E, Supplementary Fig. 3E) assay assessed that knockdown of *NFE2L3* hindered migration and invasion of Caki-1 and Caki-2 cells, while concurrent 5-Aza-CdR treatment attenuated this effect, and the level was recovered to the level of the sh-NC group. In summary, knockdown of *NFE2L3* repressed malignant behaviors of ccRCC cells, and demethylation treatment substantially fostered malignant phenotypes of ccRCC cells by increasing *NFE2L3* expression.

**Fig. 4** Repression of methylation attenuates the tumor suppressive effect caused by *NFE2L3* knockdown in Caki-1 cells. **A** qRT-PCR detected Caki-1 cell transfection efficiency; **B** Western blot detected the protein expression of *NFE2L3* in transfected Caki-1 cells; **C** Cell colony formation assay detected proliferative ability of Caki-1 cells; **D** Scratch healing assay detected the migratory ability of Caki-1 cells ( $\times 40$ ); **E** Cell invasion assay detected the invasive ability of Caki-1 cells ( $\times 100$ ). (\* denotes  $p < 0.05$ )



## Discussion

As the subtype with the highest incidence of renal cancer, ccRCC is characterized by difficulty in early screening and poor prognosis after surgery. So far, specific drugs targeting ccRCC have not been developed, and the molecular mechanism controlling the malignant progression of ccRCC remains unclear. Here, we demonstrated the association between *NFE2L3* and ccRCC and high expression of *NFE2L3* in ccRCC. The hypomethylation of *NFE2L3* regulated its high gene expression, thus promoting the proliferation, migration, and invasion of cancer cells.

We first proved that *NFE2L3* could facilitate malignant phenotypes of ccRCC cells via bioinformatics analysis and a series of in vitro assays. Ralf Küppers et al. confirmed

high expression of *NFE2L3* in Hodgkin's lymphoma by large-scale gene expression profiling and validation of gene expression in Hodgkin's lymphoma cells [20]. In addition to hematopoietic malignancies, *NFE2L3* mRNA level was also reported to be elevated in breast cancer cells [21]. These studies are in line with this study. In addition, *NFE2L3* usually functions as a transcription factor to regulate tumor growth. It can regulate the expression of cell cycle-related genes to promote cell proliferation [11], which has been relatively well studied in colon cancer. For example, some scholars found that *NFE2L3* transcription factor plays a key role in the pathway connecting NF- $\kappa$ B signal and CDK1 activity control, thus promoting the proliferation of colon cancer cells [17]. This may provide an idea for our follow-up study on the mechanism of *NFE2L3*



promoting the development of ccRCC. However, the roles of *NFE2L3* in different cancers are different. *NFE2L3* also functions as a repressor in other cancer types. For example, *NFE2L3* can inhibit the development of lymphoma [10], inconsistent with our study. The specific molecular mechanism of *NFE2L3* upregulation in ccRCC was studied in depth. Epigenetic changes are vital in tumor initiation and progression and can be used as tumor markers [22, 23]. Global methylation dysregulation and methylation phenotypes in CpG islands have also been widely observed in some cancer studies [24]. Bioinformatics prediction has found that *NFE2L3* may serve as a new DNA methylation driver gene and prognostic marker in ccRCC [16], which was also confirmed in our study. *NFE2L3* was hypomethylated in ccRCC patient tissues and cell lines. Although degree of methylation of *NFE2L3* in the ccRCC cell line Caki-2 was noticeably lower compared to RPTEC, the methylated and unmethylated levels of *NFE2L3* in Caki-2 cells were almost equal. It was not completely consistent with protein expression levels, possibly because *NFE2L3* expression could be affected by factors other than methylation. For example, *NFE2L3* is a target of miR-23b-3p in colon adenocarcinoma [25] and a target of miR-1246 in breast cancer [26]. Hence, *NFE2L3* expression in ccRCC cell lines may also be regulated by multiple miRNAs, which needs future studies.

However, whether the upregulation of *NFE2L3* expression is caused by dysregulation of methylation level has not been demonstrated experimentally. That is why we explore this issue further. We treated ccRCC cells with methylation inhibitor with gradient concentrations and then detected the expression level of *NFE2L3*. Our results proved that in LoMet-ccRCC, Caki-2 and 769-P cell lines, expression increased dependently on concentration of methylation inhibitor. Demethylation treatment had little effect on Caki-1 cells with extremely low *NFE2L3* methylation. In other words, *NFE2L3* level was closely associated with methylation degree in the gene promoter region. This is in line with earlier studies illustrating that activating genes with carcinogenic potential through DNA hypomethylation promotes the development of cancer [27]. We further unveiled that demethylation treatment substantially attenuated the repressive effect of *NFE2L3* knockdown on cell malignant behavior in ccRCC. This suggested that the *NFE2L3* upregulation promoting ccRCC development was activated by DNA hypomethylation.

At present, research on DNA methylation is not extensive, and scholars generally believe that DNA methylation will be a new target in cancer research and therapy. In the present study, regulation of hypomethylated *NFE2L3* on ccRCC was studied. We hope we can provide new ideas for ccRCC therapy and therefore improve ccRCC patients' prognoses.

**Supplementary Information** The online version contains supplementary material available at <https://doi.org/10.1007/s12033-023-00727-w>.

**Author Contributions** All authors contributed to data analysis, drafting, and revising the article, gave final approval of the version to be published, and agreed to be accountable for all aspects of the work.

**Funding** Not applicable.

**Data Availability** The data used to support the findings of this study are included within the article.

## Declarations

**Competing interests** The authors declare no conflict of interest.

**Ethical Approval** The study was approved by the ethics committee of People's Hospital of Lishui City.

**Research Involving Human and Animals Rights** Not applicable.

## References

1. Siegel, R. L., Miller, K. D., & Jemal, A. (2018). Cancer statistics, 2018. *CA: A Cancer Journal for Clinicians*, 68, 7–30. <https://doi.org/10.3322/caac.21442>
2. Cohen, H. T., & McGovern, F. J. (2005). Renal-cell carcinoma. *New England Journal of Medicine*, 353, 2477–2490. <https://doi.org/10.1056/NEJMra043172>
3. Shaw, G. (2016). The silent disease. *Nature*, 537, S98–99. <https://doi.org/10.1038/537S98a>
4. Chowdhury, I., Mo, Y., Gao, L., Kazi, A., Fisher, A. B., & Feinstein, S. I. (2009). Oxidant stress stimulates expression of the human peroxiredoxin 6 gene by a transcriptional mechanism involving an antioxidant response element. *Free Radical Biology & Medicine*, 46, 146–153. <https://doi.org/10.1016/j.freeradbiomed.2008.09.027>
5. Andrews, N. C. (1998). The NF-E2 transcription factor. *International Journal of Biochemistry & Cell Biology*, 30, 429–432. [https://doi.org/10.1016/s1357-2725\(97\)00135-0](https://doi.org/10.1016/s1357-2725(97)00135-0)
6. Chevillard, G., & Blank, V. (2011). NFE2L3 (NRF3): The Cinderella of the Cap'n'Collar transcription factors. *Cellular and Molecular Life Sciences*, 68, 3337–3348. <https://doi.org/10.1007/s00018-011-0747-x>
7. Derjuga, A., Gourley, T. S., Holm, T. M., Heng, H. H. Q., Shivdasani, R. A., Ahmed, R., Andrews, N. C., & Blank, V. (2004). Complexity of CNC transcription factors as revealed by gene targeting of the Nrf3 locus. *Molecular and Cellular Biology*, 24, 3286–3294. <https://doi.org/10.1128/MCB.24.8.3286-3294.2004>
8. Braun, S., Hanselmann, C., Gassmann, M. G., Keller, U. A. D., Born-Berclaz, C., Chan, K., Kan, Y. W., & Werner, S. (2002). Nrf2 transcription factor, a novel target of keratinocyte growth factor action which regulates gene expression and inflammation in the healing skin wound. *Molecular and Cellular Biology*, 22, 5492–5505. <https://doi.org/10.1128/MCB.22.15.5492-5505.2002>
9. Xiao, Q., Pepe, A. E., Wang, G., Luo, Z., Zhang, Li., Zeng, L., Zhang, Z., Yanhua, Hu., Ye, S., & Qingbo, Xu. (2012). Nrf3-Pla2g7 interaction plays an essential role in smooth muscle differentiation from stem cells. *Arteriosclerosis, Thrombosis, and Vascular Biology*, 32, 730–744. <https://doi.org/10.1161/ATVBAHA.111.243188>
10. Chevillard, G., Paquet, M., & Blank, V. (2011). Nfe2l3 (Nrf3) deficiency predisposes mice to T-cell lymphoblastic

- lymphoma. *Blood*, 117, 2005–2008. <https://doi.org/10.1182/blood-2010-02-271460>
11. Masudul Azad Chowdhury, A. M., Katoh, H., Hatanaka, A., Iwanari, H., Nakamura, N., Hamakubo, T., Natsume, T., Waku, T., & Kobayashi, A. (2017). Multiple regulatory mechanisms of the biological function of NRF3 (NFE2L3) control cancer cell proliferation. *Scientific Reports*, 7, 12494. <https://doi.org/10.1038/s41598-017-12675-y>
  12. Gonzalo, S. (2010). Epigenetic alterations in aging. *Journal of Applied Physiology*, 1985(109), 586–597. <https://doi.org/10.1152/jappphysiol.00238.2010>
  13. Wang, Y. P., & Lei, Q. Y. (2018). Metabolic recoding of epigenetics in cancer. *Cancer Communications (Lond)*, 38, 25. <https://doi.org/10.1186/s40880-018-0302-3>
  14. Shen, Z., Zhu, L., Zhang, C., Cui, X., & Lu, J. (2019). Overexpression of BHLHE41, correlated with DNA hypomethylation in 3'UTR region, promotes the growth of human clear cell renal cell carcinoma. *Oncology Reports*, 41, 2137–2147. <https://doi.org/10.3892/or.2019.7004>
  15. Kang, H. W., Park, H., Seo, S. P., Byun, Y. J., Piao, X. M., Kim, S. M., Kim, W. T., Yun, S. J., Jang, W., Shon, H. S., & Ryu, K. H. (2019). Methylation signature for prediction of progression free survival in surgically treated clear cell renal cell carcinoma. *Journal of Korean Medical Science*, 34, e144. <https://doi.org/10.3346/jkms.2019.34.e144>
  16. Jie Wang, Hu., Zhao, H. D., Zhu, L., Wang, S., Wang, P., Ren, Q., Zhu, H., Chen, J., Lin, Z., Cheng, Y., Qian, B., Zhang, Yi., Jia, R., Weizheng, Wu., Jun, Lu., & Tan, J. (2019). LAT, HOXD3 and NFE2L3 identified as novel DNA methylation-driven genes and prognostic markers in human clear cell renal cell carcinoma by integrative bioinformatics approaches. *Journal of Cancer*, 10, 6726–6737. <https://doi.org/10.7150/jca.35641>
  17. Bury, M., Le Calvé, B., Lessard, F., Dal Maso, T., Saliba, J., Michiels, C., Ferbeyre, G., & Blank, V. (2019). NFE2L3 controls colon cancer cell growth through regulation of DUX4, a CDK1 inhibitor. *Cell Reports*, 29(1469–1481), e1469. <https://doi.org/10.1016/j.celrep.2019.09.087>
  18. Wang, X., Li, Y., Fang, Z., & Li, Y. (2021). Elevated expression of NFE2L3 promotes the development of gastric cancer through epithelial-mesenchymal transformation. *Bioengineered*, 12, 12204–12214. <https://doi.org/10.1080/21655979.2021.2005915>
  19. Ren, Y., Wang, Y., Hao, S., Yang, Y., Wendong Xiong, Lu., & Qiu, J. T. (2020). Aifa Tang NFE2L3 promotes malignant behavior and EMT of human hepatocellular carcinoma (HepG2) cells via Wnt/betacatenin pathway. *Journal of Cancer*, 11, 6939–6949. <https://doi.org/10.7150/jca.48100>
  20. Küppers, R., Klein, U., Scherwing, I., Distler, V., Bräuninger, A., Cattoretti, G., Yuhai, Tu., Stolovitzky, G. A., Califano, A., Hansmann, M.-L., & Dalla-Favera, R. (2003). Identification of Hodgkin and Reed-Sternberg cell-specific genes by gene expression profiling. *Journal of Clinical Investigation*, 111, 529–537. <https://doi.org/10.1172/JCI16624>
  21. Rhee, D. K., Park, S. H., & Jang, Y. K. (2008). Molecular signatures associated with transformation and progression to breast cancer in the isogenic MCF10 model. *Genomics*, 92, 419–428. <https://doi.org/10.1016/j.ygeno.2008.08.005>
  22. Shen, H., & Laird, P. W. (2013). Interplay between the cancer genome and epigenome. *Cell*, 153, 38–55. <https://doi.org/10.1016/j.cell.2013.03.008>
  23. Ren, X., Yang, X., Cheng, B., Chen, X., Zhang, T., He, Q., Li, B., Li, Y., Tang, X., Wen, X., Zhong, Q., Kang, T., Zeng, M., Liu, Na., & Ma, J. (2017). HOPX hypermethylation promotes metastasis via activating SNAIL transcription in nasopharyngeal carcinoma. *Nature Communications*, 8, 14053. <https://doi.org/10.1038/ncomms14053>
  24. Viren Amin, R., Harris, A., Onuchic, V., Jackson, A. R., Charnecki, T., Paithankar, S., Subramanian, S. L., Riehle, K., Coarfa, C., & Milosavljevic, A. (2015). Epigenomic footprints across 111 reference epigenomes reveal tissue-specific epigenetic regulation of lincRNAs. *Nature Communications*, 6, 6370. <https://doi.org/10.1038/ncomms7370>
  25. Huang, G., Yang, Y., Lv, M., Huang, T., Zhan, X., & Yao, Y. (2021). Jianghou Hou miR-23b-3p Inhibits the oncogenicity of colon adenocarcinoma by directly targeting NFE2L3. *Journal of Oncology*, 2021, 8493225. <https://doi.org/10.1155/2021/8493225>
  26. Dai, Y. C., Pan, Y., Quan, M. M., Chen, Q., Pan, Y., Ruan, Y. Y., & Sun, J. G. (2021). MicroRNA-1246 mediates drug resistance and metastasis in breast cancer by targeting NFE2L3. *Frontiers in Oncology*, 11, 677168. <https://doi.org/10.3389/fonc.2021.677168>
  27. Feinberg, A. P., & Tycko, B. (2004). The history of cancer epigenetics. *Nature Reviews Cancer*, 4, 143–153. <https://doi.org/10.1038/nrc1279>

**Publisher's Note** Springer Nature remains neutral with regard to jurisdictional claims in published maps and institutional affiliations.

Springer Nature or its licensor (e.g. a society or other partner) holds exclusive rights to this article under a publishing agreement with the author(s) or other rightsholder(s); author self-archiving of the accepted manuscript version of this article is solely governed by the terms of such publishing agreement and applicable law.